Mouse Strain Differences in Plasmacytoid Dendritic Cell Frequency and Function Revealed by a Novel Monoclonal Antibody

Carine Asselin-Paturel,[1] Géraldine Brizard, Jean-Jacques Pin, Francine Brière, and Giorgio Trinchieri

We report in this study the generation of a novel rat mAb that recognizes mouse plasmacytoid dendritic cells (pDC). This Ab, named 120G8, stains a small subset of CD11c^{low} spleen cell with high specificity. This population produces high amounts of IFN-α upon in vitro viral stimulation. Both ex vivo- and in vitro-derived 120G8^{+} cells display a phenotype identical with that of the previously described mouse pDC (B220^{high}Ly6C^{high}Gr1^{low}CD11b^{-}CD11c^{low}). Mice treated with 120G8 mAb are depleted of B220^{high}Ly6C^{high}CD11c^{low} cells and have a much-reduced ability to produce IFN-α in response to in vivo CpG stimulation. The mAb 120G8 stains all and only B220^{high}Ly6C^{high}CD11c^{low} pDC in all lymphoid organs. Immunohistochemical studies performed with this mAb indicate that pDC are located in the T cell area of spleen, lymph nodes, and Peyer's patches. Although the Ag recognized by 120G8 is not yet known, we show that its expression is up-regulated by type I IFN on B cells and DC. Using this mAb in immunofluorescence studies demonstrates strain- and organ-specific differences in the frequency of pDC and other DC subsets. 129Sv mice have a much higher frequency of pDC, together with a lower frequency of conventional CD8α^{+}CD11c^{high} DC, compared with C57BL/6 mice, both in spleen and blood. The higher ability of 129Sv mice to produce IFN-α in vivo is related to a higher number of pDC, but also to a higher ability of pDC from 129Sv mice to produce IFN-α in vitro in response to viral stimulation. *The Journal of Immunology*, **2003, 171: 6466–6477.**

Dendritic cells (DC)[2] are APCs that initiate T cell-dependent immune responses (1). In humans, plasmacytoid DC (pDC) are a DC subset characterized by their ultrastructural resemblance to Ig-secreting plasma cells, their unique surface phenotype (CD4^{+}IL-3R^{high}CD45RA^{+}HLA^{-}DR^{+}) (2, 3), and by their ability to produce high levels of IFN-α in response to virus stimulation (4, 5) or to oligodeoxynucleotides (ODN) containing particular CpG motifs (6). Human pDC also differ from conventional myeloid DC in their weak phagocytic activity (3, 7), their weak IL-12 production capacity (8), and the signals inducing their activation (6). The two DC subtypes make different links between acquired and innate immune responses, with conventional DC activating both B cells (9) and NK cells (10), and pDC producing large amounts of natural IFNs in response to viruses (11). Human natural IFN-producing cells (IPC) have also been shown to play an essential role in activating NK cells to kill virus-infected cells (12).

In the mouse, pDC have been identified as CD11c^{low}B220^{high} Gr1^{low} cells, able to produce IFN-α in response to viral stimulation and exhibiting plasmacytoid morphology (13–15). Mouse pDC can also be obtained in large number, both in vitro by differentiating bone marrow cells into DC in the presence of FMS-like tyrosine kinase (FLT)3 ligand (16, 17), and in vivo (18).

Human pDC have been shown to induce potent in vitro priming and Th1 polarization of naive T cells following viral encounter (19–21). Plasmacytoid DC have also been shown to induce IL-10 secreting T cells (8, 22) and CD8^{+} regulatory T cells (23). Indeed, the nature of the T cell response upon presentation of Ag by DC is dependent on the subpopulation of DC involved, the Ag dose, the cytokine environment, and on the stage of maturation of presenting DC (24, 25). In addition, due to their functional plasticity, conventional DC and pDC are able to polarize the type of the T cell response toward a Th1 or a Th2 response, in part through their capacity to secrete IL-12 or not, respectively (8, 25).

In humans, resting pDC have been shown to specifically express blood DC Ag (BDCA)-2 and BDCA-4 (26). In mouse models, no such specific markers have been identified to date. It would be of great benefit to identify new markers specific for mouse pDC to monitor, characterize, and isolate pDC and also to study their function in vivo in animal models. Type I IFNs (IFN-α, -β, or -ω) are central players in host resistance to viral or microbial infections (27, 28). Furthermore, human pDC have been recently associated with inflammatory diseases, in particular in lupus erythematosus lesions (29) and nasal mucosa of airway allergy (30). The critical role of pDC in IFN type I production during viral infections has been recently demonstrated in vivo, in murine CMV and vesicular stomatitus virus infection models (31, 32). However, anti-Gr1 treatment, used to deplete pDC and demonstrate the role of this subset in murine CMV infection (31, 32), can also, in addition to neutrophils, deplete a proportion of macrophages and of activated T cells (31).

The present study describes the generation of such a mouse pDC-specific rat mAb, designated as 120G8. This mAb stains pDC from either ex vivo total cells or in vitro bone marrow-derived DC.

Laboratory for Immunological Research, Schering-Plough Research Institute, Dardilly, France

Received for publication July 7, 2003. Accepted for publication October 1, 2003.

The costs of publication of this article were defrayed in part by the payment of page charges. This article must therefore be hereby marked *advertisement* in accordance with 18 U.S.C. Section 1734 solely to indicate this fact.

[1] Address correspondence and reprint requests to Dr. Carine Asselin-Paturel, Schering-Plough, Laboratory for Immunological Research, 27 chemin des Peupliers, F-69571 Dardilly, France. E-mail address: carine.paturel@spcorp.com

[2] Abbreviations used in this paper: DC, dendritic cell; pDC, plasmacytoid DC; ODN, oligodeoxynucleotide; BDCA, blood DC Ag; IPC, IFN-α producing cell; MFI, mean fluorescence intensity; FLT, FMS-like tyrosine kinase; PALS, periarteriole lymphoid site.

0022-1767/03/$02.00

It also recognizes pDC originating not only from different organs in the mouse, but also from different mouse strains. Finally 120G8 mAb injection in vivo depletes mice of pDC, as determined both phenotypically and functionally. Use of this Ab enabled us to demonstrate some mouse strain-specific differences in pDC frequency and IFN-α response, both in vitro and in vivo.

Materials and Methods

Mice, culture medium, and Abs

Specific pathogen-free female BALB/c AnN, 129SvPas, C3H/HeN, CBA/J, C57BL/6J, DBA/2J, BALB/c SCID mice and BALB/c ByJ-v/v (nude) mice, 6–10 wk of age, were purchased from Charles River Laboratories (L'Arbresle, France). IFN type I receptor knockout mice (A129) were purchased from B&K Universal (London, U.K.) and bred at the Charles River animal facility. All mice experiments were performed following protocols approved by the institutional animal committee and in accordance with European Economic Community Council Directive 86/609 as well as institutional animal care and use guidelines.

Primary cells were cultured in complete medium: RPMI 1640 (Life Technologies, Paisley Park, U.K.) supplemented with 10% (v/v) heat-inactivated FCS (Life Technologies), 2 mM L-glutamine (Life Technologies), 80 μg/ml gentallin (Schering-Plough, Union, NJ), 10 mM HEPES (Life Technologies), 50 μM 2-ME (Sigma-Aldrich, St. Louis, MO), at 37°C in 5% CO_2. All Abs were from BD PharMingen (San Diego, CA), unless otherwise specified.

Rat immunization with mouse pDC

One rat LOU female (Charles River Laboratories) at 4-wk-old was immunized with sorted spleen mouse $CD11c^+Gr1^+CD11b^-CD9^-DX5^-CD3\epsilon^-$ cells (pDC) and isolated as previously described (13) from BALB/c mice between 6 and 8 wk of age. Once sorted, cells were washed three times in PBS (Life Technologies), resuspended in PBS, and frozen at −20°C until time of injection. The protocol of immunization was the following: day 0, i.p. injection of 10^6 cells in CFA; day 14, i.p. injection of 10^6 cells in IFA; day 21, i.p. injection of 10^6 cells in PBS; day 35, i.v. injection of 2×10^6 cells in PBS; day 38, rat was sacrificed and spleen was collected. Splenocytes were fused with the murine myeloma cell line SP_2O, using polyethylene glycol 1000 (Sigma-Aldrich). Hybrid cells were plated in 96-well plates and fed with DMEM F12 (Life Technologies) supplemented with 10% (v/v) horse serum (Life Technologies), 2 mM L-glutamine (Life Technologies), 80 μg/ml gentallin (Schering-Plough), 1% culture medium additive (EFS, Lyon, France), 10^{-5} M azaserine (Sigma-Aldrich), and 5×10^{-5} M hypoxanthine (Sigma-Aldrich). Supernatant fluids were screened for reactivity with isolated total spleen cells, bone marrow, and spleen $CD11c^+$ DC. Selected hybridomas were cloned by limiting dilution. The selected hybridoma, named 120G8, was further grown in DMEM F12 (Life Technologies) supplemented with 10% (v/v) horse serum (Life Technologies), 2 mM L-glutamine (Life Technologies), 80 μg/ml gentallin (Schering-Plough). Ab was purified from supernatant fluid of 120G8 cell culture without serum, by anion-exchange chromatography on Hiload Q column (Pharmacia Biotech, Uppsala, Sweden). Purified Ab was labeled with Alexa 488 and biotin using corresponding labeling kits, according to the manufacturer's instructions (Molecular Probes, Leiden, The Netherlands). Ig isotype was determined by ELISA using a rat Ig subtyping kit (BD PharMingen).

Tissue preparation and cell depletion

Mice were killed by CO_2 inhalation. Isolated cells were maintained throughout the procedure in cold PBS (Life Technologies) supplemented with 5% (v/v) heat-inactivated FCS and 0.5 mM EDTA (Sigma-Aldrich) (PBS-FCS-EDTA). Blood cells were collected in excess PBS-FCS-EDTA. Spleens, lymph nodes (popliteal and mesenteric) were crushed in cold PBS-FCS-EDTA and passed through a 25-gauge needle. Bone marrow cells were flushed out of the bones with cold PBS-FCS-EDTA. Thymuses were incubated in collagenase (Sigma-Aldrich) for 30 min at 37°C, and then were crushed in cold PBS-FCS-EDTA and passed through a 25-gauge needle. For all samples, RBC were lysed in NH_4Cl solution (StemCell Technologies, Vancouver, British Columbia, Canada) for 5 min at 4°C.

FACS analysis

For all FACS analysis, cells were first incubated for 30 min at 4°C in the presence of rat anti-CD16/32 (2.4G2) Ab to ensure blocking of Fc receptors. Stained cells were analyzed with a FACScan flow cytometer (BD Biosciences, Mountain View, CA). Negative controls were performed with corresponding rat Ig. When possible, autofluorescent cells were gated out using the FL3 channel.

For study of 120G8 specificity, isolated total spleen cells from BALB/c mice were stained with 120G8-Alexa 488 and PE-labeled Abs (hamster anti-CD3ϵ (145-2C11) or anti-CD11c (HL-3), rat anti-CD19 (1D3) or anti-pan NK cells (DX5) for 30 min at 4°C. Surface phenotyping of $120G8^+$ cells was performed on either freshly isolated DC ($CD11c^+$ cells purified from total spleen cells by positive selection using $CD11c^+$ Microbeads and MiniMacs (Miltenyi Biotec, Bergisch Gladbach, Germany) or in vitro-derived DC (bone marrow cells incubated for 8–9 days in 25 ng/ml recombinant murine FLT3 ligand (R&D Systems, Abingdon, U.K.), as previously described (16, 17). Both population of DC were stained for 20 min at 4°C with 120G8-Alexa 488, hamster anti-CD11c-allophycocyanin and either PE-labeled Abs (anti-CD45R/B220, Ly6G/C, CD11b, I-A^b, H2-K^b, CD8α) or biotin-labeled anti-Ly6C, further revealed with streptavidin-PE (DAKO, Glostrup, Denmark).

For analysis of Gr1 expression on $120G8^+$ cells, freshly isolated DC from BALB/c ($CD11c^+$ cells purified by positive selection using Macs columns (Miltenyi Biotec) were first incubated in the presence of excess (100 μg/ml) unlabeled Abs (rat anti-Ly6C, Ly6G/C (RB6-8C5) or Ly6G (1A8)), washed and then stained for 20 min at 4°C with 120G8-Alexa 488, hamster anti-CD11c-allophycocyanin and rat anti-Ly6G/C-PE Abs.

For surface phenotyping of $120G8^+$ cells in mouse organs, freshly isolated cells were stained for 20 min at 4°C with 120G8-Alexa 488, hamster anti-CD11c-allophycocyanin, anti-CD45R/B220-PE and either anti-Ly6C- or anti-Ly6G/C-biotin, followed by staining with streptavidin-PerCp-Cy5.5 (BD PharMingen).

For analysis of DC subsets frequency, isolated cells from different organs and from different mouse strains were stained for 20 min at 4°C with 120G8-Alexa 488, hamster anti-CD11c-allophycocyanin, a mixture of anti-$CD3\epsilon^-$ and anti-CD19-PerCp-Cy5.5 and either anti-CD8α-PE or anti-CD11b-PE.

Cell sorting

Isolated spleen cells were incubated for 30 min at 4°C with a mixture of rat anti-CD3 molecular complex (17A2), anti-CD8β (53-5.8), anti-CD19 (1D3), or anti-erythrocyte (TER119). Cells and goat anti-rat IgG-coated Dynabeads (Dynal Biotech, Oslo, Norway) were mixed under continuous agitation for 15 min at 4°C. Beads and attached cells were removed using a Dynal magnet. Depleted cells were stained with 120G8-Alexa 488 and hamster anti-CD11c (HL-3)-PE for 30 min at 4°C and sorted using a FACStar^{Plus} flow cytometer (BD Biosciences). Cells were washed, resuspended in complete medium, and stimulated at 0.5×10^6 cells/ml in 96-well culture plates.

In vitro cell activation

The formaldehyde-inactivated human influenza virus, strain NK/TM/138/00 kindly provided by N. Kuehn (Aventis Pasteur, Val de Reuil, France) was added to the cultures at a final concentration of 100 hemagglutinin units/ml. CpG ODN (TCA TTG GAA AAC GTT CTT CGG GGC G) was phosphorothioate-modified (MWG Biotec, Munich, Germany) and used in vitro at a final concentration of 10 μg/ml. Total spleen cells were stimulated at 10^6 cells/ml in 96-well culture plates. For analysis of cytokine production, supernatants were collected at 20 h and stored at −20°C for further analysis. Production of mouse IFN-α was determined by specific ELISA (PBL Biomedical Laboratories, New Brunswick, NJ). IL-12 p40 and IL-12 p70 production were assayed using IL-12 p70/p40 Duoset ELISA (R&D Systems) and IL-12 p70-specific Duoset ELISA (R&D Systems), respectively.

For in vitro up-regulation of 120G8, total spleen cells were cultured for 20 h in the presence of mouse IFN-γ (R&D Systems) at 20 ng/ml, mouse IFN-α (Hycult Biotechnology, Uden, The Netherlands) at 100 U/ml, influenza virus, LPS (Sigma-Aldrich) at 10 μg/ml, or R848 compound (Invivogen, San Diego, CA) at 10 μg/ml. Stimulated cells were stained with 120G8-Alexa 488 and rat anti-CD19, CD4, CD8β, DX5, or hamster anti-CD11c-PE.

In vivo treatment

For in vivo cytokine induction, mice were anesthetized and injected i.v. in the retro-orbital vein, using a glass syringe, with 200 μl of CpG with 1,2-dioleoyloxy-3-trimethylammonium-propane (DOTAP) preparation (30 μl of a cationic liposome preparation (DOTAP; Boehringer Mannheim) mixed with 5 μg of CpG ODN in 170 μl of PBS, in a polystyrene tube). Control mice received the same preparation without CpG. Mice depleted of pDC had received i.p. injection of 120G8 ascites (obtained in BALB/c nude mice) at day 1 and day 0 before CpG treatment. Mice were killed and blood was collected by cardiac punction at 6 h after CpG injection. Serum

was prepared from whole blood by coagulation for 30 min at 37°C and centrifugation. Sera were titrated for mouse IFN-α and IL-12 (p40 and p70) using ELISA (PBL Biomedical Laboratories and R&D Systems, respectively). Spleen cells were isolated at the same time to evaluate the efficiency of pDC depletion by flow cytometry (see *Materials and Methods*). Briefly, isolated cells were stained for 30 min at 4°C with anti-Ly6C-FITC, anti-CD45R/B220-PE, a mixture of anti-CD3ϵ-PerCp-Cy5.5 and anti-CD11c-allophycocyanin.

Immunohistofluorescent staining

Mouse organs were embedded in OCT compound (Miles, Elkhart, IN), snap frozen in liquid nitrogen and stored at −80°C until further analysis. Cryosections (8-μm thick) were fixed in 95% acetone (Sigma-Aldrich) at −20°C for 20 min, dried at room temperature, and stored frozen at −20°C until staining was performed. Sections were then rehydrated in PBS (Life Technologies). Avidin-biotin tissue content was neutralized using specific kit (Vector Laboratories, Burlingame, CA). Sections were first incubated with 2% normal mouse serum (DAKO) to eliminate any unspecific Ab binding. Sections were stained sequentially with unlabeled 120G8 Ab for 60 min, goat anti-rat coupled to Alexa 488 (Molecular Probes) for 60 min, 2% rat serum for 30 min, indicated Abs (rat anti-CD19 for B cells, anti-CD3 complex for T cells, anti-CD11b for macrophages and myeloid cells, hamster anti-CD11c for DC) coupled to biotin for 60 min and finally streptavidin-Alexa 594 (Molecular Probes) for 30 min. Slides were air dried and mounted under coverslips with one drop of Fluoromount G (Electron Microscopy Sciences, Fort Washington, PA). Slides were viewed on a Zeiss Axioscop epifluorescence microscope. Pictures were taken using an Optronics MagnaFire Digital Camera (Optronic, Goleta, CA). Identical sections were pictured for both fluorescence (Alexa 488 and Alexa 594) and pictures were overlaid with ImagePro Express software.

Statistical analysis

Statistical analysis of results was performed using two-tailed Student's *t* test. Results are presented as the mean ± SEM, unless otherwise indicated.

Results

Selection of mAb 120G8 reactive against mouse pDC

To study the distribution and function of mouse pDC in vitro and in vivo, mAbs that specifically recognized pDC were generated. One rat was immunized with sorted pDC, as described in *Materials and Methods*. Supernatants from resulting hybrid cells were screened by FACS staining for reactivity with less than 5% of cells of total mouse spleen cell preparations. Selected supernatants were further assayed for reactivity on both bone marrow and spleen cells enriched for $CD11c^+$ cells. Supernatant from one hybridoma, named 120G8, was found to react only with a major subset of bone marrow $CD11c^+$ cells (50–70%), and a minor $CD11c^{low}$ subset of spleen $CD11c^+$ cells (10–20% of total $CD11c^+$). The hybridoma was cloned by limiting dilution. The mAb produced by 120G8 hybridoma was found to be of IgG1/κ isotype, as determined by ELISA (data not shown). As the $120G8^+$ cells in the spleen appeared to be also $CD11c^+B220^+Gr1^+$ cells (formerly defined as mouse pDC) (13, 14), the hybridoma 120G8 was selected for further studies.

Monoclonal Abs 120G8 is highly reactive with mouse IPC (pDC)

The reactivity of 120G8 mAb was further examined on freshly isolated total spleen cells, using double immunofluorescence studies with 120G8 mAb and lineage specific markers. mAb 120G8 stained a small subset of freshly isolated spleen cells that were homogenous in forward and side scatter (data not shown). This subset did not express CD3ϵ (T cell lineage marker), CD19 (B cell lineage marker), DX5 (NK cell lineage marker) (Fig. 1*A*) or TER119 (erythrocyte lineage marker, data not shown). In contrast, all $120G8^+$ cells were $CD11c^{low}$, confirming that the Ab stained a subset of spleen DC (Fig. 1*A*). A small subset of double positive $CD3\epsilon^+120G8^+$ or $CD19^+120G8^+$ cells could sometime be detected among total spleen cells. This was most probably due to doublets of T or B cells with $120G8^+$ cells, rather than 120G8 staining of T or B cells, because all $120G8^+$ cells were found to be $CD11c^+$ DC.

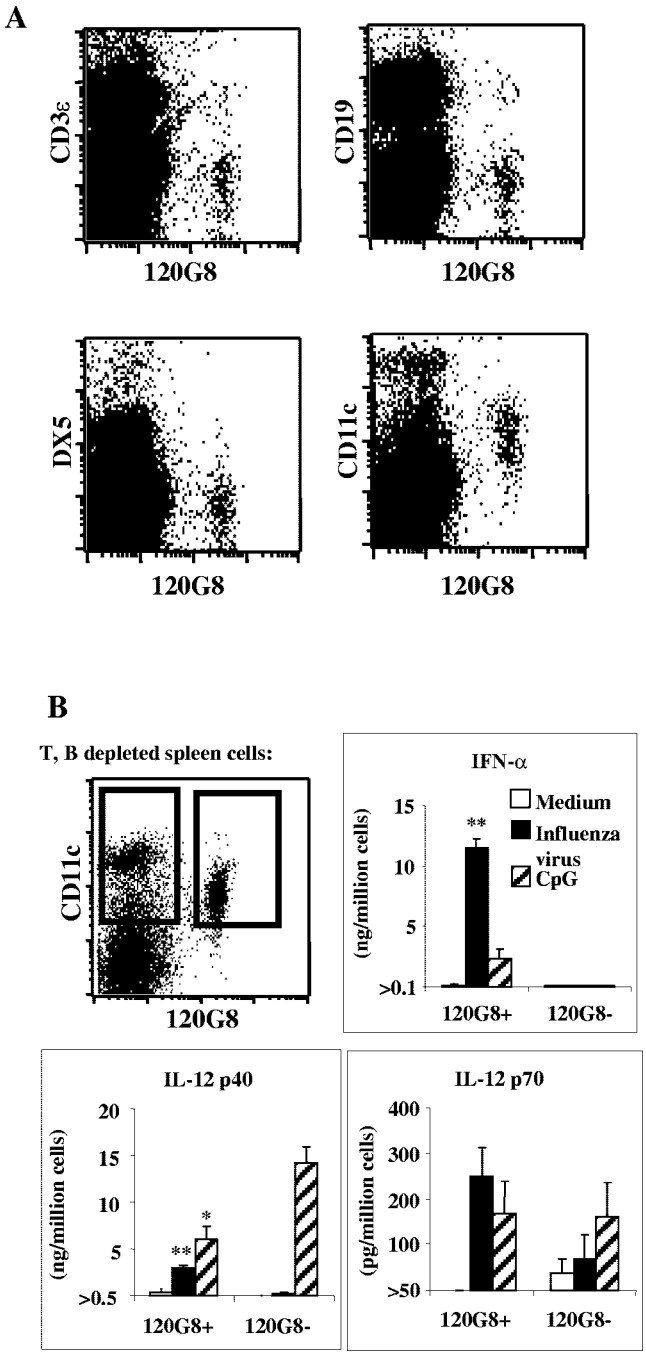

FIGURE 1. Monoclonal Ab 120G8 stains mouse spleen IPC. *A*, Total spleen cells from BALB/c mice were stained with 120G8-Alexa488 and the indicated PE-labeled Abs. Dot plots shown for each staining are representative of at least three determinations in separate experiments. *B*, Spleen cells from 129Sv mice were depleted for T cells and B cells and stained as described in *Materials and Methods*. Both $120G8^+CD11c^+$ and $120G8^-CD11c^+$ populations were selected as shown in *B* and stimulated with medium, inactivated influenza virus, or CpG ODN. Culture supernatants were collected after 20 h and assayed for IFN-α, IL-12p70 and p40 by ELISA. Mean cytokine concentration (± SEM) of at least three experiments is shown; *, $p < 0.05$, **, $p < 0.01$, compared with $120G8^-$ cells.

Next, the ability of 120G8 mAb to specifically recognize IPC was tested in vitro. $CD11c^+$ cells have already been shown to be

the only spleen cells to produce high amounts of IFN-α in vitro in response to influenza virus stimulation (13). $CD11c^+120G8^+$ and $CD11c^+120G8^-$ cells were sorted by flow cytometry from spleen cells depleted of $CD3^+$, $CD19^+$, $CD8\beta^+$, and $TER119^+$ cells. The two subsets were further stimulated in vitro by inactivated influenza virus or CpG ODN. Only the $120G8^+$ subset of $CD11c^+$ cells produced IFN-α after both influenza virus and CpG ODN stimulation (Fig. 1*B*). IFN-α production by $120G8^-$ sorted cells in response to both influenza virus and CpG was always below detection levels. Following influenza virus stimulation, $120G8^+$ cells were also secreting higher IL-12 p40 levels than was the $120G8^-$ subset, while producing lower levels of this cytokine than $120G8^-$ cells, in response to CpG (Fig. 1*A*). This was also true for IL-12 p70 production, although not statistically significant, due to production level often close to detection limit.

Surface phenotype of $120G8^+CD11c^+$ spleen and bone marrow-derived cells

Mouse pDC have been previously described to be $CD11c^{low}$ $Gr1^+B220^+$ cells in the spleen (13), and $CD11c^+B220^+CD11b^-$ cells among DC derived in vitro from bone marrow cells in the presence of FLT3 ligand (17). Surface phenotype of $120G8^+$ cells, in comparison with $120G8^-$ DC, was analyzed on ex vivo isolated $CD11c^+$ spleen cells and DC derived in vitro from bone marrow cells in FLT3 ligand. DC derived from bone marrow in GM-CSF, known to inhibit pDC development (17), did not stain for 120G8 mAb (data not shown). Ex vivo spleen $120G8^+$ cells were $CD11c^{low}$, $B220^{high}$, $Gr1^{low}$, $Ly6C^{high}$, $CD11b^-$, $H\text{-}2K^{d+}$, $IA^{d/low}$, and $CD8\alpha^{-/low}$, whereas $CD11c^+120G8^-$ cells were $B220^{-/low}$, $Gr1^-$, $Ly6C^{-/low}$, $CD11b^{+/-}$, $H\text{-}2K^{d+}$, $IA^{d/low/high}$, and $CD8\alpha^{+/-}$ (Fig. 2*A*). Surface phenotype of $120G8^+$ cells corresponds to the previously described surface phenotype of mouse spleen pDC (13–15). When FLT3 ligand-stimulated bone marrow cell cultures were analyzed, $120G8^+$ cells were $B220^{high}$, $Gr1^{-/low}$, $Ly6C^{high}$, $CD11b^-$, $H\text{-}2K^{d+}$, $IA^{d/low}$ and $CD8\alpha^-$, whereas $120G8^-$ cells were $B220^-$, $Gr1^-$, $Ly6C^-$, $CD11b^+$, $H\text{-}2K^{d+}$, $IA^{d/low}$, and $CD8\alpha^-$ (Fig. 2*B*). This surface phenotype of in vitro-derived $120G8^+$ cells correspond to that previously described for in vitro-derived pDC phenotype (16). Thus, 120G8 mAb stains both mouse spleen pDC and in vitro-derived pDC. Furthermore, 120G8 mAb stained $CD11c^+CD11b^-B220^+$ cells throughout the bone marrow-derived culture in FLT3 ligand, although it never stained $CD11c^-$ cells (data not shown), suggesting that 120G8 mAb is an early marker of mouse pDC along their in vitro differentiation.

In vivo depletion of $120G8^+$ cells abrogates IFN-α production

In previous studies, the role of pDC in viral infections has been demonstrated by depleting those cells with anti-Ly6G/C (Gr1) treatment. This treatment, in addition to pDC and neutrophils, also possibly depletes a proportion of macrophages and of activated T cells. Thus the use of 120G8 to deplete specifically pDC could be of great use for in vivo studies. To assess the effect of 120G8 depletion on IFN-α production, 129Sv mice, previously treated or not with 120G8 mAb were injected i.v. with CpG ODN, as described in *Materials and Methods*. Serum IFN-α, IL-12 p40, and IL-12 p70 production were assayed at the peak of IFN-α production, 6 h after CpG treatment. Control sera from mice injected i.v. with diluent instead of CpG were negative for all cytokines tested (data not shown). Treatment with 120G8 completely abrogated IFN-α production induced by CpG treatment and partially inhibits both IL-12 p40 and IL-12 p70 production (Fig. 3*A*). Thus, 120G8 mAb depletes IPC in vivo.

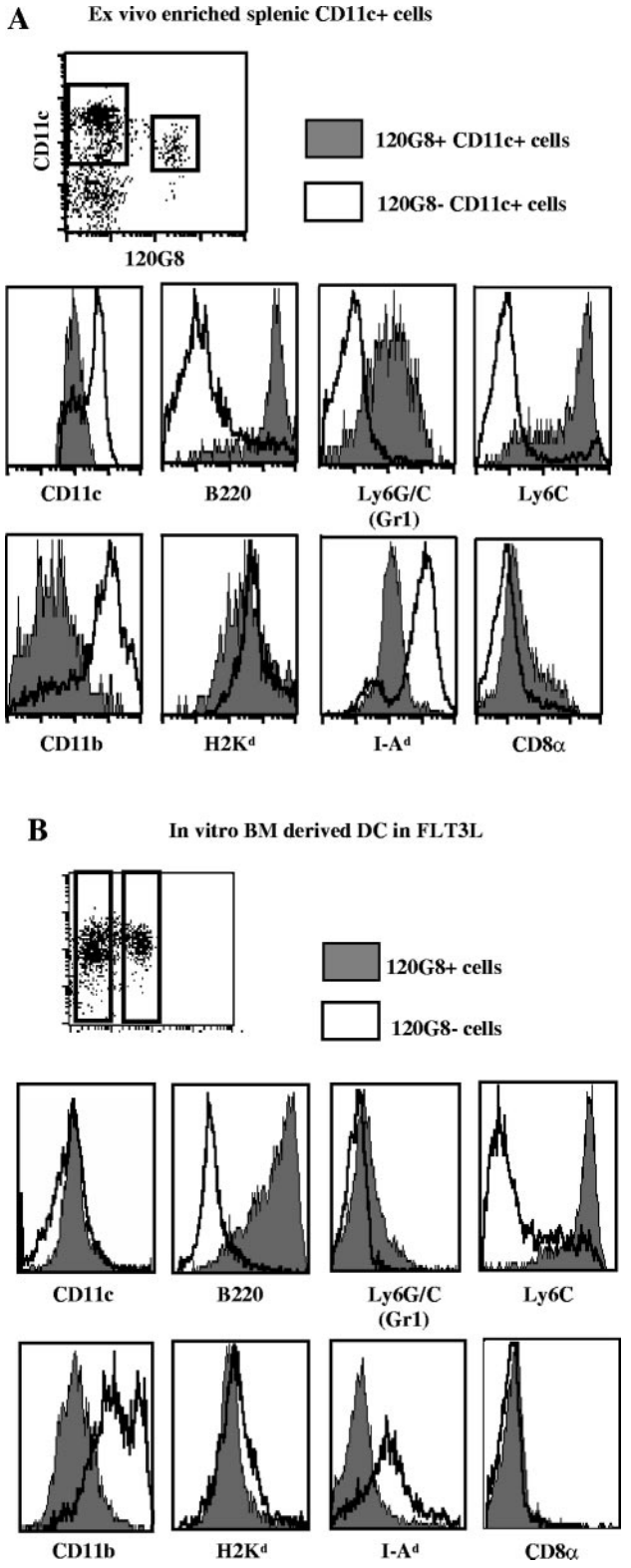

FIGURE 2. Surface phenotype of $120G8^+$ cells. Isolated spleen $CD11c^+$ cells (*A*) and in vitro-derived DC (*B*) were obtained and stained as described in *Materials and Methods*. Filled histograms show staining with indicated PE-labeled Abs on $120G8^+$ DC cells gated (*top left panel*) and open histograms show staining with indicated PE-labeled Abs on $120G8^-$ DC cells gated (*top left panel*). Data shown for each staining are representative of at least two determinations in separate experiments. The *x*-axis of the histograms indicates the MFI in a logarithmic scale (from 10^0 to 10^4) whereas the *y*-axis indicates with an arbitrary unit in a linear scale the number of cells acquired.

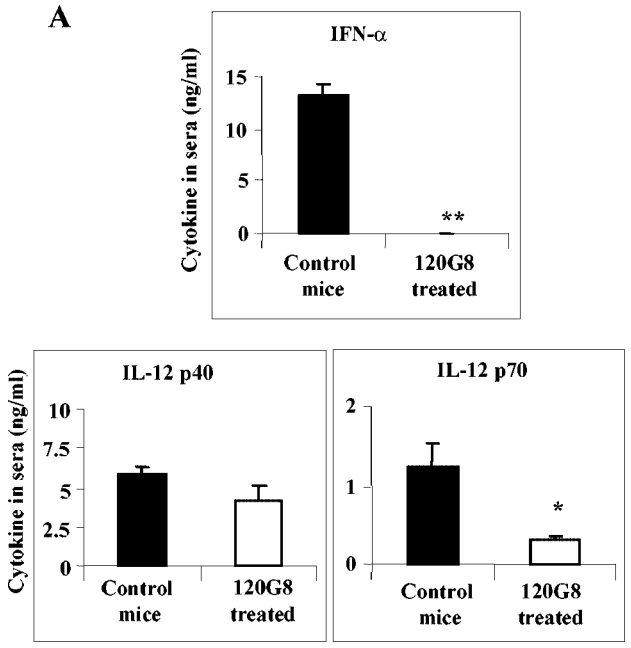

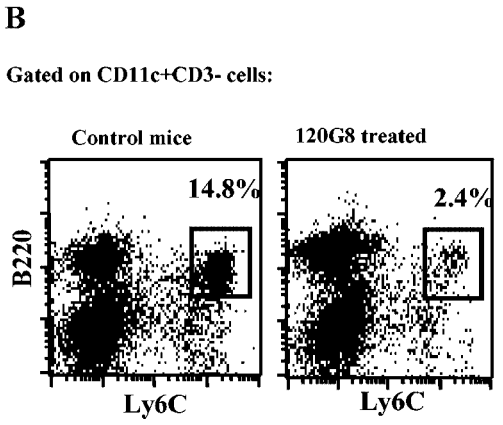

FIGURE 3. In vivo depletion of 120G8$^+$ cells abrogates IFN-α production. *A*, Sera from untreated or 120G8-treated 129Sv mice were collected 6 h after i.v. injection of CpG plus DOTAP preparation (as described in *Materials and Methods*) and titrated for IFN-α and IL-12. The sera of the mice injected with DOTAP alone were negative for IFN-α and IL-12. Mean cytokine concentration ($\pm$ SEM) of three mice in each group are shown; $*$, $p < 0.05$, $**$, $p < 0.01$, compared with untreated mice. Similar results were obtained in three independent experiments. *B*, Spleen cells from untreated or 120G8-treated BALB/c mice were collected 24 h after Ab treatment and stained as described in *Materials and Methods*. Dot plot is shown for selected CD3ϵ^-CD11c$^{low/high}$ cells and percentage of B220^{high}Ly6C^{high} cells among gated cells is given for one representative mice of three. Experiment was performed twice.

To assess the efficiency of pDC depletion in vivo, mice were injected i.p. or not with 120G8 mAb. After 24 h, spleen cells were analyzed by FACS analysis for the presence of Ly6C$^+$B220$^+$CD11c$^+$CD3$^-$ cells. Indeed, one single in vivo injection with 120G8 mAb decreased the frequency of spleen Ly6C$^+$B220$^+$CD11c$^+$ cells (pDC) by ~80% (Fig. 3*B*).

Mouse pDC do not express the Ly6G Ag

Mouse pDC have been shown to express Gr1 (13, 14), previously known as a granulocyte-specific marker (33). The RB6-8C5 Ab (Gr1) reacts strongly with neutrophil-specific Ly6G Ag, but it has also been described to cross-react with the Ly6C Ag (34), expressed on monocytes/macrophages, activated T cells, and NK cells (35–37). As mouse pDC also strongly express the Ly6C Ag and to determine whether pDC do really express the Ly6G Ag, we studied the staining of 120G8$^+$ cells with a new Ab specific to Ly6G, clone 1A8. The 120G8$^+$ cells did not stain for Ly6G-specific Ab (Fig. 4*A*). To further elucidate the Gr1 staining observed on mouse pDC, we performed competitive binding to 120G8$^+$ cells between anti-Ly6G/C (Gr1) mAb and either anti-Ly6C, anti-Ly6G/C, or anti-Ly6G specific Abs. Only preincubation with excess anti-Ly6C, and to a lower extent, anti-Ly6G/C specific Ab prevented Gr1 staining on 120G8$^+$ cells, but not the staining with anti-Ly6G specific Ab (Fig. 4*B*). Inhibition of Ly6G/C (Gr1) staining could still be detected after preincubation with as low as 0.5 μg/ml anti-Ly6C Ab (data not shown), confirming that pDC staining by Gr1 Ab is mostly due to the cross-reactivity of this Ab with Ly6C Ag.

Monoclonal Abs 120G8 stains all, and is restricted to, CD11c$^+$Ly6C$^+$B220$^+$ cells

Mouse pDC have been formerly identified as CD11c$^+$B220^{high}Gr1^{low}Ly6C^{high} cells in the spleen and other immune organs (13, 14). To demonstrate that 120G8 mAb recognizes

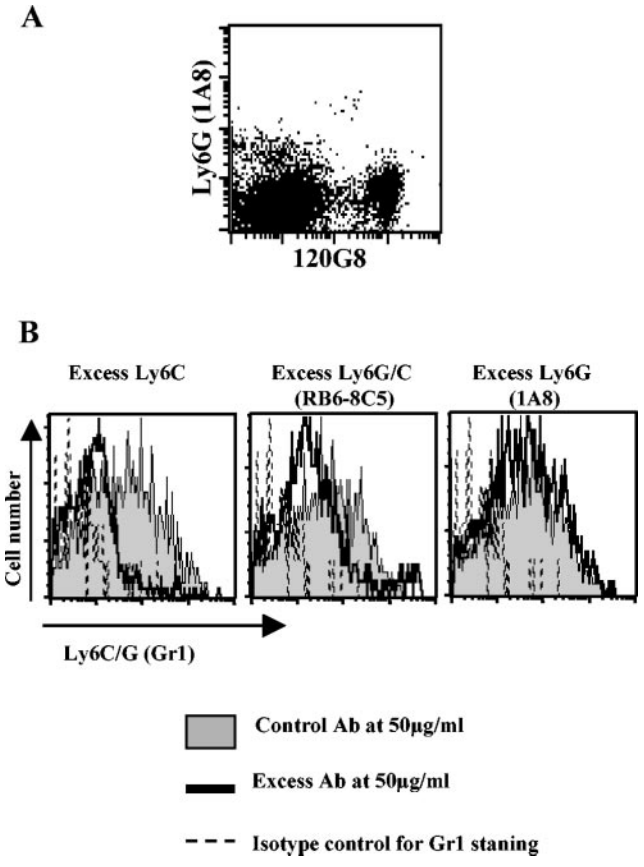

FIGURE 4. Gr1 expression on 120G8$^+$ cells. *A*, Purified spleen CD11c$^+$ cells from BALB/c mice were stained with 120G8-biotin and anti-Ly6G (1A8)-FITC, followed by streptavidin-PE staining. The dot plot shown is representative of two experiments. *B*, Spleen CD11c$^+$ cells from BALB/c mice were incubated with an excess (50 μg/ml) of control (filled histograms) or indicated Abs (open histograms, straight line) and further stained with anti-Ly6G/C(Gr1)-PE. Dotted-line histograms represent isotype-PE staining. Data shown are representative of two independent experiments.

all mouse pDC in all organs and only those cells, isolated cells from various organs were analyzed in quadruple surface staining with 120G8, anti-CD45R/B220, anti-CD11c, and either anti-Ly6C or anti-Gr1 Abs. In the spleen, all 120G8$^+$ cells were found to be B220^{high}Ly6C^{high} (Fig. 5*A*). Reciprocally, when B220^{high}Ly6C^{high} spleen cells were gated, they were found to represent two distinct populations, one expressing both CD11c and 120G8, and the other being negative for both markers (presumably a minor population of B cells expressing Ly6C or T cells expressing B220) (Fig. 5*A*). The staining of 120G8 mAb was also investigated in bone marrow, blood, peripheral lymph node, and thymus from BALB/c mice. In those samples, 120G8$^+$ cells were all B220$^+$Ly6C$^+$, as well as B220$^+$Ly6G/C^{low}, although the levels of Ly6G/C and B220 expression appeared to vary, depending on the organ of origin of the pDC (Fig. 5*B*). Reciprocally when B220^{high}Ly6C^{high} cells were analyzed, as in the spleen, they represented two distinct populations, one CD11c^{low} that was also 120G8$^+$, and the other CD11c$^-$ that was also 120G8$^-$ (Fig. 5*B*). Similar results were obtained in all immune and also other nonimmune organs tested (data not shown). These results demonstrate that 120G8 mAb can recognize mouse pDC (defined as CD11c$^+$B220$^+$Ly6C$^+$) cells, regardless from which tissue they have been isolated.

Immunohistochemical staining of 120G8 on tissue section

The in situ distribution of pDC was next examined using 120G8 mAb staining on tissue sections (Fig. 6). In all organs tested, 120G8$^+$ individual cells could be detected, that double stained for both B220 and Ly6C Ags (data not shown), confirming data obtained by FACS staining. However, double-staining of 120G8$^+$ cells with CD11c Ab, as described in *Materials and Methods*, could not be performed, due to low expression of CD11c on mouse pDC (data not shown). Thus only conventional CD11b$^+$ and CD8α^+CD11c^{high} DC could be detected with the CD11c staining used in this study. In some organs (e.g., thymus), some lower 120G8 staining on endothelial cells could also be detected. In spleen, 120G8$^+$ cells were not located in B cell area (Fig. 6*A*). In fact, pDC were seen both in the inner periarteriole lymphoid site (PALS; T cell area, Fig. 6*B*), and in the red pulp, with only very few pDC in the marginal zone (Fig. 6*C*). This distribution of mouse pDC contrasted with conventional CD11c^{high} DC that were mostly located in the outer PALS (Fig. 6*D*). Mouse pDC localization in the T cell area was also observed in tissue section from peripheral (Fig. 6*E*) or mesenteric lymph node (data not shown), as well as for Peyer's patches (Fig. 6*F*). However in the absence of T cells, as is the case in SCID mice, most of the pDC still did not colocalize with marginal zone macrophages (Fig. 6*G*), but displayed similar distribution to conventional CD11c^{high} DC (Fig. 6*H*).

Expression of 120G8 is up-regulated on B cells in the presence of type I IFN

The data presented demonstrate that 120G8 mAb specifically stains mouse pDC among total cells from normal mice. We further investigated whether cytokine activation could induce 120G8 up-regulation on other immune cells. Total spleen cells were isolated, incubated 24 h in vitro in the presence of cytokines and 120G8 staining was analyzed on B, T CD4$^+$, T CD8$^+$, NK cells, macrophages, CD11c^{high} DC, and pDC. Type I IFNs, but not type II IFN or other cytokines tested (IL-12, TNF-α, data not shown), induced an up-regulation of 120G8 staining only on B cells and DC, whereas no effect was detected on T, NK, and macrophages (Fig. 7*A*, data not shown for macrophages). However the mean fluorescence intensity (MFI) of 120G8 staining on B cells or DC still remained at least one log lower than on pDC. Moreover, 120G8 staining remained constant on type I IFN-activated pDC (Fig. 7*A*).

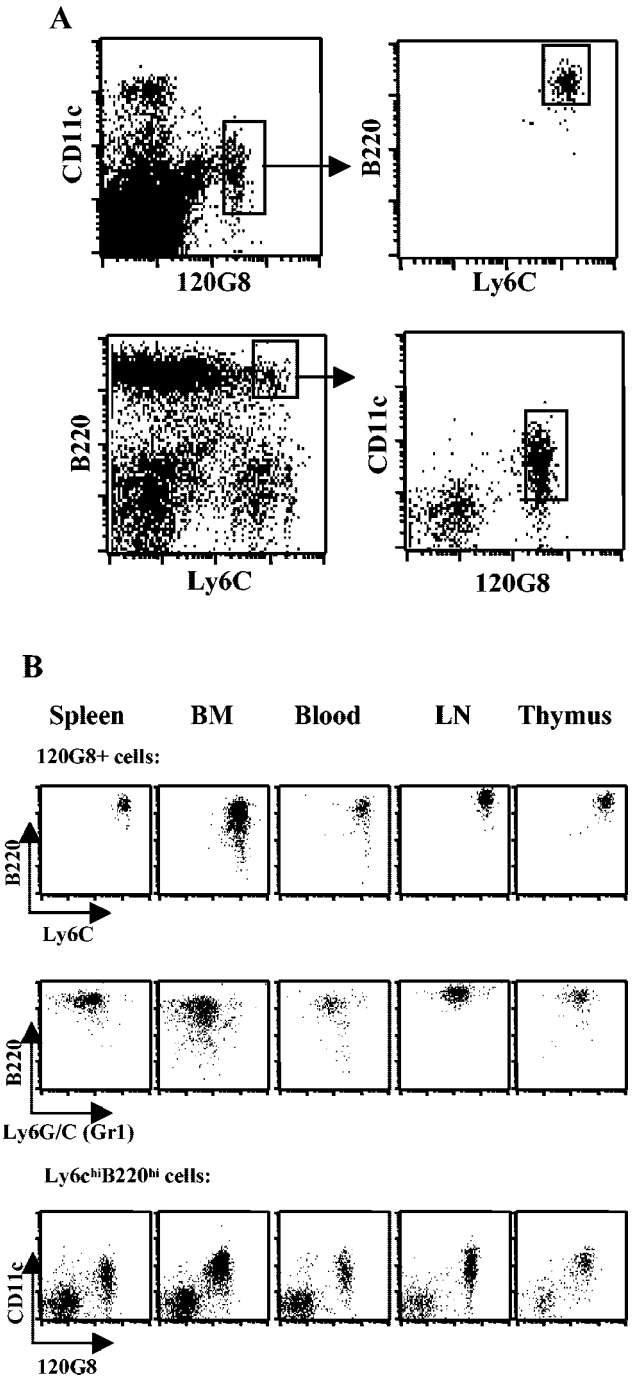

FIGURE 5. 120G8 recognizes B220$^+$Ly6C$^+$CD11c$^+$ cells in immune organs. *A*, Spleen cells from BALB/c mice were isolated and stained as described in *Materials and Methods*. Staining with anti-B220 and anti-Ly6C is shown in the *right upper panel* for selected 120G8$^+$CD11c$^+$ cells (as shown in the *left upper panel*). Staining with anti-CD11c and 120G8 is shown in the *right lower panel* for selected B220^{high}Ly6C^{high} cells (as shown in the *left lower panel*). Data representative of two experiments are shown. *B*, Cells from BALB/c mice were isolated from the indicated organs and stained as described in *Materials and Methods*. In the *top* and *middle panels*, 120G8$^+$ cells staining with anti-B220 and either anti-Ly6C (*top panels*) or anti-Ly6G/C (*middle panels*) is shown. In the *bottom panels*, B220^{high}Ly6C^{high} cells staining with anti-CD11c and 120G8 is shown.

Consistent with this observation, stimuli known to induce or activate IFN type I signaling pathway, such as R848, LPS, CpG, poly(I:C), or influenza virus also induced 120G8 up-regulation on

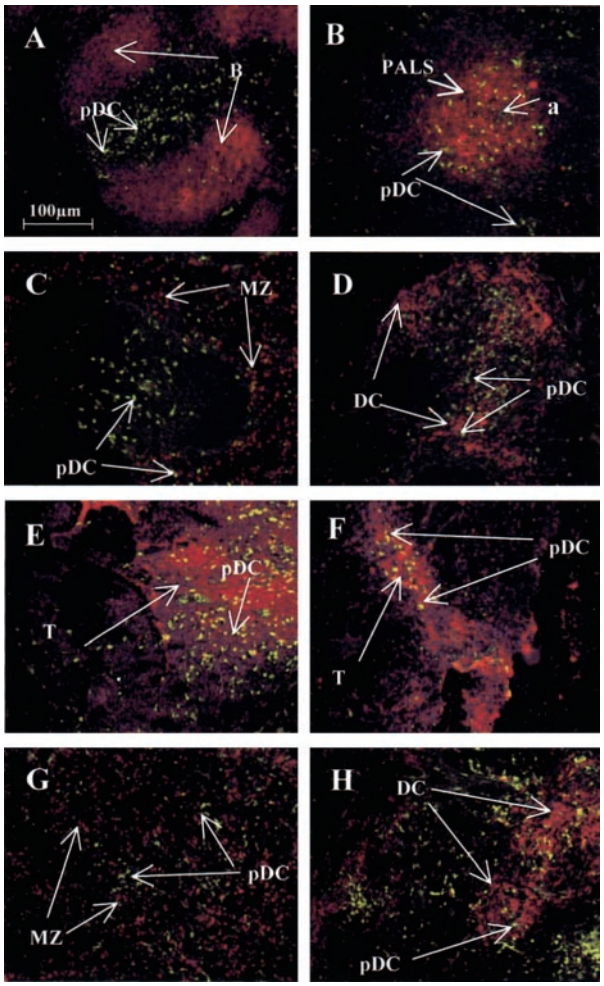

FIGURE 6. 120G8$^+$ cell localization in mouse immune organs. Mouse tissue sections were obtained and stained as described in *Materials and Methods*. Seriated spleen sections from BALB/c mice were costained with 120G8 in green and in red: anti-CD19 (*A*), anti-CD3 complex (*B*), anti-CD11b (*C*), and anti-CD11c (*D*) Abs. Peripheral lymph node (*E*) and Peyer's patches (*F*) sections were costained with 120G8 in green and anti-CD3 complex Ab in red. Spleen sections from SCID mice were costained with 120G8 in green and in red: anti-CD11b (*G*), and anti-CD11c (*H*) Abs. Overlaid images of the two fluorescence on identical sections are shown. pDC, Plasmacytoid 120G8$^+$ cells; B, B cell zone; a, Arteriole; MZ, Marginal zone; DC, Conventional CD11c^{high} DC; T, T cell zone.

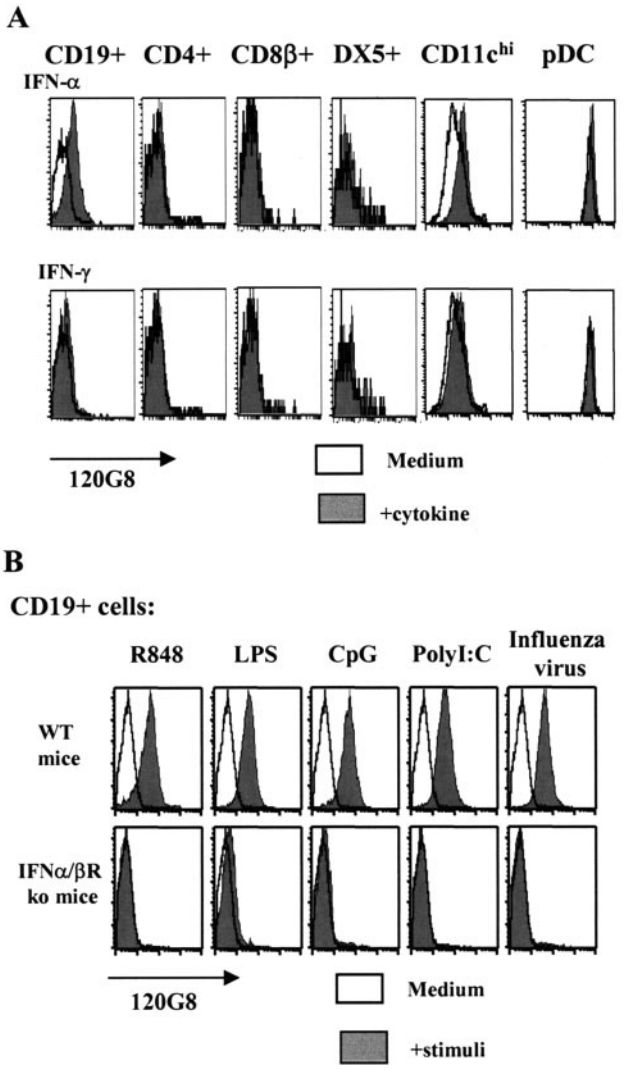

FIGURE 7. Expression of 120G8 on activated spleen cells. Total spleen cells were isolated from 129Sv wild-type mice or IFN-$\alpha\beta$ R knockout mice, and stimulated with medium (open histograms) or the indicated cytokines (*A*) or stimuli (*B*) (filled histograms). Staining with 120G8 mAb on the indicated gated cells is shown, representative of at least two separate experiments. The *x*-axis of the histograms indicates the MFI in a logarithmic scale (from 10^0 to 10^4) whereas the *y*-axis indicates with an arbitrary unit in a linear scale the number of cells acquired.

B cells (Fig. 7*B*) and DC (data not shown). However, in the absence of IFN type I receptor, this up-regulation was abrogated (Fig. 7*B*, data not shown for DC). Under those conditions, no significant regulation of 120G8 expression on pDC could be detected in wild-type mice (data not shown). Moreover, pDC isolated from IFN-$\alpha\beta$ receptor knockout mice still expressed 120G8, although at a lower level than wild-type mice (pDC, 120G8 MFI = 124.7 ± 2.5 for wild-type mice vs 95.33 ± 4.2 for IFN-$\alpha\beta$ receptor knockout mice, $p = 0.0006$; 120G8$^-$ DC, 120G8 MFI = 6.1 ± 1.8 for wild-type mice vs 5.3 ± 0.2 for IFN-$\alpha\beta$ receptor knockout mice, $p = 0.26$). This demonstrates that 120G8 expression on resting pDC is only marginally dependent on IFN type I signaling.

Frequency of 120G8$^+$ cells in different mouse strains

The ability of 120G8 mAb to react with pDC from different mouse strains was investigated. This Ab reacted with spleen pDC isolated from BALB/cByJ, 129 SvPas, C57BL/6J, CBA/J, C3H/HeN, and DBA/2J mice. However, when spleen cells from C57BL/6 and 129Sv mice were analyzed their respective frequency of CD19$^-$CD3$^-$CD11c^{high}CD11b$^+$ (conventional CD11b$^+$ DC), CD19$^-$CD3$^-$CD11c^{high}CD8α^+ (conventional CD8$^+$ DC) and CD19$^-$CD3$^-$CD11c^{low}120G8$^+$ cells (pDC), the C57/Bl6 mice exhibited a significantly lower pDC frequency among DC compared with 129Sv mice (6.7% ± 2.6 vs 27.8% ± 4.2, $p = 2.3 \times 10^{-6}$) (Fig. 8*A*). This discrepancy was also true when pDC frequency among total spleen cells was analyzed (Fig. 8*B*). In contrast, CD8α^+ DC were found to be present at a higher frequency among total DC in C57BL/6 mice than in 129Sv mice (20.2 ± 2.6% vs 5.1 ± 2.2%, $p = 4.3 \times 10^{-7}$). Comparable frequencies of conventional CD11b$^+$ DC among total DC were found in both strains, although slightly lower in 129Sv mice (Fig. 8*A*).

The frequency, among total spleen cells and popliteal lymph node cells, of the three DC subsets was further investigated for six different mouse strains. In spleen, this analysis showed that not only the frequency of total DC among total spleen cells but also pDC and conventional CD11c^{high}CD8α^+ subsets frequency

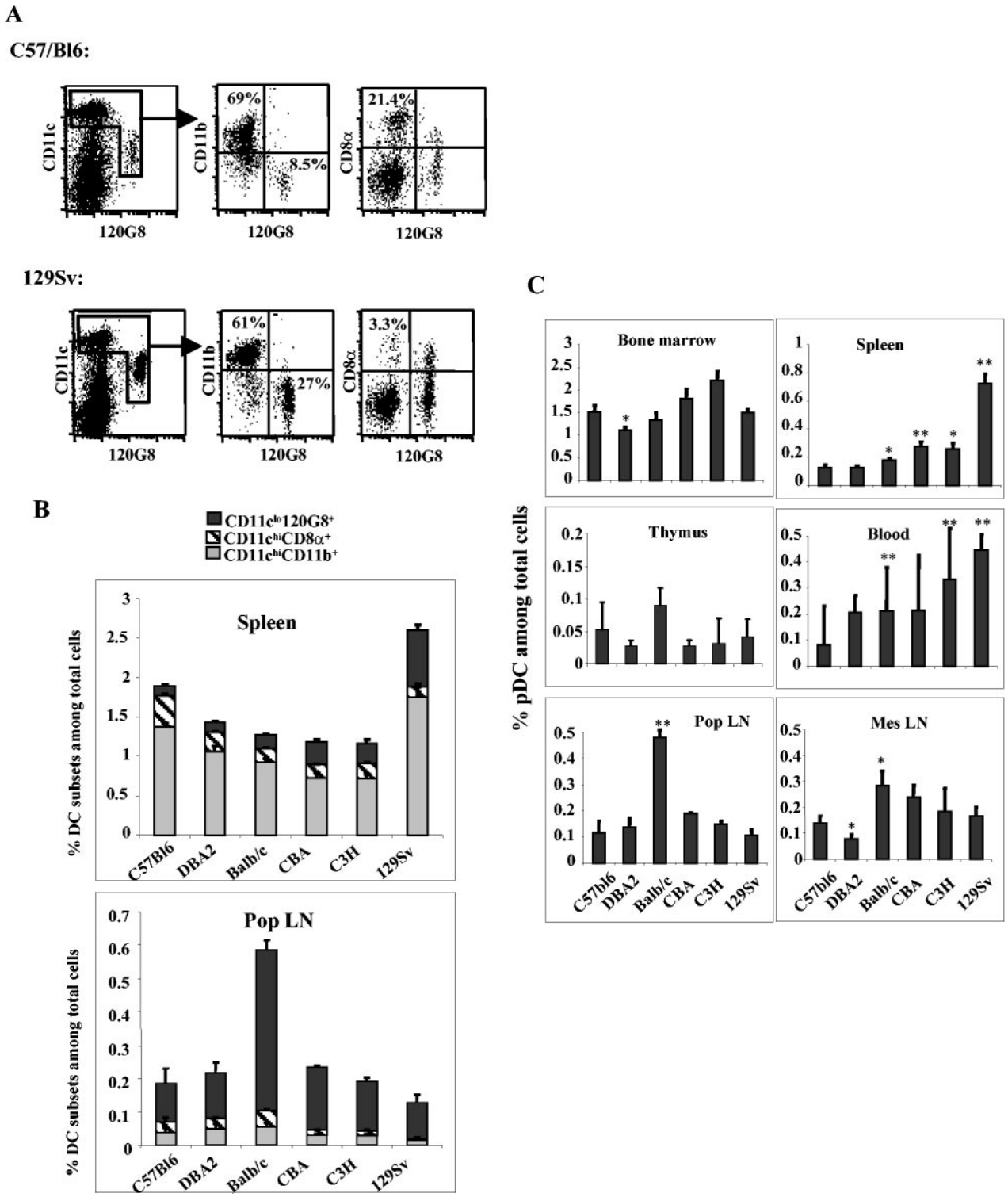

FIGURE 8. Mouse DC subsets frequency in immune organs. *A*, Total spleen from C57BL/6 mice (*upper panels*) or 129Sv mice (*lower panels*) were isolated and stained as described in *Materials and Methods*. Three mice per mouse strain were used. Conventional DC ($CD11c^{high}$) and pDC ($120G8^+CD11c^{low}$) were gated among $CD19^-CD3\epsilon^-$ cells, as shown in the two *left panels*. Anti-CD11b, anti-CD8a, and 120G8 staining on those selected DC are shown in the *middle* and *right panels*. Data are shown for one representative mouse of nine mice from a total of three independent experiments. *B*, Total spleen and popliteal lymph node cells from mice of indicated mouse strain were isolated and stained as described in *Materials and Methods*. Conventional $CD11b^+$ DC ($CD19^-CD3\epsilon^-CD11c^{high}CD11b^+$), conventional $CD8^+$ DC ($CD19^-CD3\epsilon^-CD11c^{high}CD8\alpha^+$), and pDC ($CD19^-CD3\epsilon^-CD11c^{low}120G8^+$) mean percentage among total cells (± SEM) of at least six mice (two independent experiments giving similar results) is shown. *C*, Total cells from the indicated organs were isolated and stained as described in *Materials and Methods*. Plasmacytoid DC ($CD19^-CD3\epsilon^-CD11c^{low}120G8^+$) mean percentage among total cells (± SEM) of at least six mice (from two independent experiments giving similar results) is shown. *, $p < 0.05$; **, $p < 0.01$, compared with C57BL/6 mice.

among DC varies depending on which mouse strain is considered, whereas $CD11c^{high}CD11b^{+}$ subset showed no striking difference in terms of frequency among DC (Fig. 8*B*). Interestingly, the frequency of pDC seemed to follow the reciprocal range of variation compared with the frequency of $CD11c^{high}CD8\alpha^{+}$ DC. The variation of conventional $CD11b^{+}$ DC among total spleen cells followed the variation of total DC frequency. In popliteal lymph node, all mouse strains but BALB/c mice exhibited comparable frequency of three DC subsets (mouse pDC, $CD11b^{+}$ DC, and $CD8^{+}$ DC). In contrast, in BALB/c mice, strikingly higher pDC frequency was observed, whereas conventional $CD11b^{+}$ DC and $CD8\alpha^{+}$ DC frequencies displayed no significant differences with other mouse strains (Fig. 8*B*).

When other immune organs were analyzed for pDC frequency, only blood pDC were found to display the same variation in frequency than spleen pDC (Fig. 8*C*). Bone marrow pDC showed no significant difference in frequency among the different mouse strain, as well as thymus. As previously mentioned, BALB/c popliteal lymph node pDC displayed a much higher pDC frequency than the other strains. Mesenteric lymph node pDC displayed no such striking difference between all mouse strains, although BALB/c mice still displayed the highest pDC frequency (Fig. 8*C*).

The 129Sv mouse produced a higher level of IFN-α in response to viral stimulation

To determine whether the different pDC frequency between C57BL/6 and 129Sv mice had physiologic relevance, we analyzed the ability of those two mouse strains to produce cytokines, both in vivo and in vitro. In vivo, CpG-induced secretion of IFN-α, IL-12 p40, and IL-12 p70 were significantly higher in 129Sv mice, compared with either BALB/c or C57BL/6 mice (Fig. 9*A*). In vitro, total spleen cells from 129Sv mice produced a much higher level of IFN-α and IL-12 p40 in response to both influenza virus and CpG stimulation, compared with total spleen cells from C57BL/6 mice (Fig. 9*B*). IL-12 p70 level was below detection level under those conditions. CpG stimulation on sorted pDC from both mouse strains induced comparable levels of IFN-α production and a slightly higher, although not significant, level of IL-12 in 129Sv mice (Fig. 9*C*). However, sorted pDC from 129Sv mice displayed a significantly higher cytokine production (both IFN-α and IL-12) in response to in vitro stimulation with inactivated influenza virus, compared with sorted pDC from C57BL/6 mice (Fig. 9*C*).

Discussion

This study describes the characterization and the use of a new monoclonal rat Ab that recognizes mouse plasmacytoid DC. Although two specific markers of resting naive human pDC, BDCA-2 and BDCA-4, have recently been described (26), no such markers have been described to date on mouse pDC, thus greatly impairing the study of in vivo function of pDC. The rat mAb 120G8, described in this study, specifically recognizes mouse pDC among total spleen cells. Indeed, only $120G8^{+}$ spleen cells are able to produce high amounts of IFN-α in response to both viral and CpG stimulation in vitro, and in vivo depletion of $120G8^{+}$ cells abrogates IFN-α production in response to CpG, although depletion of pDC was only ~80% efficient. The maximum of pDC depletion following i.p. injection of 120G8 mAb in vivo was seen at 24 h after injection and pDC frequency in spleen started to increase as early as 48 h after Ab treatment (data not shown). The depletion of pDC (using either 120G8 or Gr1 mAbs) could be detected in both blood and spleen, but to a much lower extent in the bone marrow or in the lymph nodes, regardless of the type or the amount of Ab used (data not shown). This could be either due to a low in vivo availability of these Abs in those specific organs, leading to incomplete cell depletion, or to a very tight regulation of pDC homeostasis in vivo. Plasmacytoid DC have been shown to display a very low turnover rate in vivo in resting conditions compared with other DC subsets (38). It still remains to be determined whether, in specific conditions as artificial depletion using 120G8 Ab or in vivo activation, the turnover rate of the pDC subset could be increased.

The observation that $120G8^{+}$ cells are also able to produce higher levels of both IL-12 p70 and IL-12 p40 than $120G8^{-}$ DC in response to viral stimulation is consistent with our previous published data (13, 31). This further suggests that pDC play a central role in viral infection, because they are the major DC subset to respond and produce cytokines in response to viral stimulation. This is also the case for other cytokines such as IL-6 and TNF-α, in response to influenza virus (data not shown) or murine CMV (39). In contrast, although only $120G8^{+}$ pDC were able to produce IFN-α in response to CpG stimulation, both $120G8^{+}$ and $120G8^{-}$ DC populations produced IL-12p40 and p70 in response to CpG. In vivo, depletion of pDC had only a minor effect on IL-12 production, both p40 and p70, in response to CpG, compared with the drastic effect on IFN-α production, further suggesting that in vivo, other cells are also able to produce IL-12 in response to CpG. This observation fits with an expression of Toll-like receptor 9 on all mouse DC subsets, at least at the mRNA level (40). Thus, depending on the nature of the stimuli, distinct DC subsets may be the major cytokine producers. Plasmacytoid DC are the preferential DC subset responding to viral infection, whereas conventional $CD8\alpha^{+}$ DC preferentially respond to other stimuli, e.g., the soluble extract from *Toxoplasma gondii* (41, 42). Moreover, Dalod et al. (39) have shown that, in the absence of pDC, the $CD11b^{+}$ DC subset was able to compensate for the production of IL-12 in response to murine CMV infection. However to date, among total DC, only pDC have been shown to produce high amounts of type I IFNs.

The $120G8^{+}$ cell displays similar phenotype to previously described mouse pDC. In particular, they have a lower level of expression of MHC class II than conventional DC, both on ex vivo isolated and in vitro-derived cells. However the level of MHC class I expression are similar in both populations, suggesting that, although resting mouse pDC have a lower ability to stimulate naive T $CD4^{+}$ T cells (25), they may be as efficient as other DC subsets in $CD8^{+}$ T cells stimulation. Our data also show that in vitro bone marrow-derived pDC and $CD11b^{+}$ DC have also similar low levels of CD11c, whereas ex vivo isolated spleen conventional DC display higher level of CD11c than pDC. This discrepancy is also observed between DC from bone marrow and blood ($CD11c^{low}$) vs conventional DC from lymph node or spleen ($CD11c^{high}$). In contrast, pDC, even when activated, remains $CD11c^{low}$ in all immune organs tested so far, suggesting that although the expression level of CD11c might be regulated on conventional DC along their in vivo maturation, this is not the case for pDC.

The expression of Gr1 Ag on mouse pDC has been lately controversial. Indeed, the Gr1 mAb (clone RB6-8C5) reacts strongly with neutrophil-specific Ly6G Ag, but it has also been described to cross-react with the Ly6C Ag, expressed on monocytes/macrophages, activated T cells, and NK cells (34). The study presented demonstrates that Ly6G/C staining on mouse pDC is not due to Ly6G Ag expression on mouse pDC (because $120G8^{+}$ cells are not stained with Ly6G-specific mAb, clone 1A8), but rather to a cross-reaction of the anti-Gr1 Ab with Ly6C Ag, which is also highly expressed on pDC. Indeed, Gr1 staining on pDC can be abrogated in the presence of an excess amount of anti-Ly6C Ab.

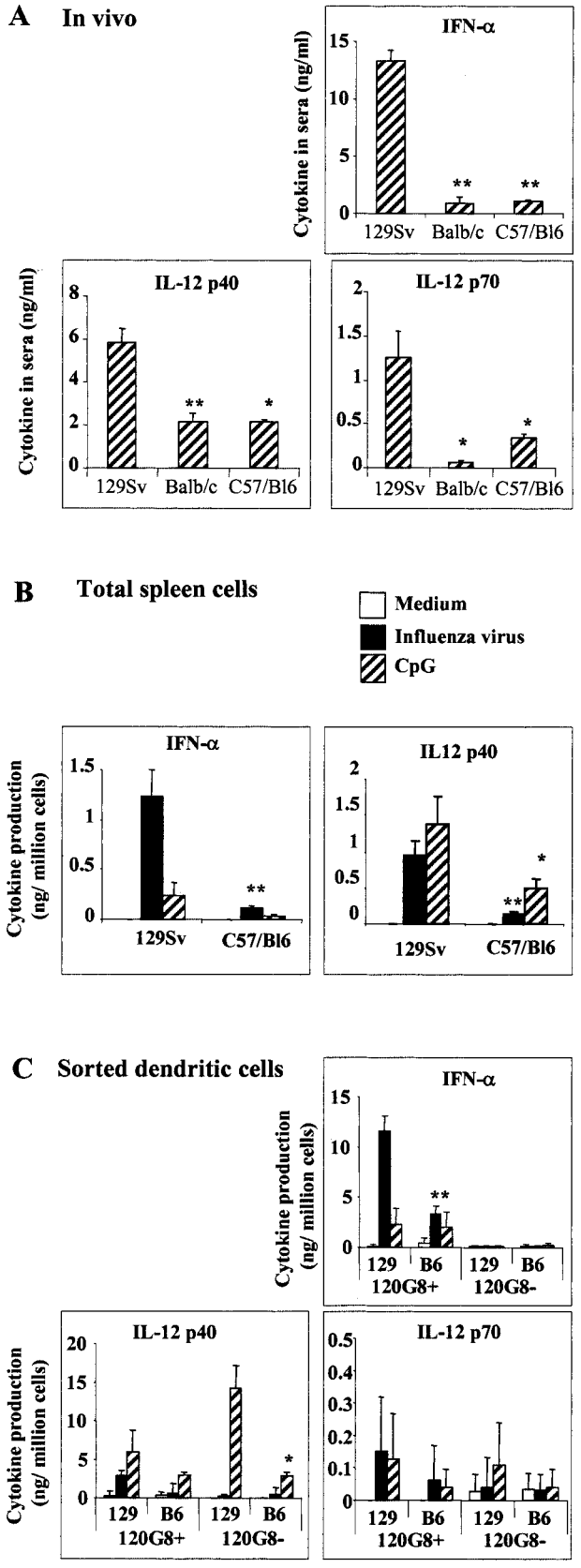

FIGURE 9. IFN-α and IL-12 production by pDC from 129Sv and C57BL/6 mice. *A*, Sera from 129Sv, BALB/c, and C57BL/6 mice were collected 6 h after CpG plus DOTAP preparation i.v. injection (as described in *Materials and Methods*) and titrated for IFN-α and IL-12 by ELISA. The sera of mice injected with DOTAP alone were negative for IFN-α and IL-12. Mean cytokine concentration ($\pm$ SEM) of three mice in each group is shown; *, $p < 0.05$, **, $p < 0.01$, compared with 129Sv mice. Similar results were obtained in two independent experiments. *B* and *C*, Total spleen cells (*B*) or sorted 120G8$^+$CD11c$^+$ and 120G8$^-$CD11c$^+$ populations (*C*) from 129Sv and C57BL/6 mice were in vitro stimulated with medium, inactivated influenza virus or CpG. Culture supernatants were collected after 20 h and assayed for IFN-α, IL-12p70, and IL-12 p40 by ELISA. Culture supernatants were collected after 20 h and assayed for IFN-α, IL-12 p70 and p40 by ELISA. Mean cytokine concentration ($\pm$ SEM) of at least three experiments is shown; *, $p < 0.05$, **, $p < 0.01$, compared with 129Sv mice.

The identification and study of activated human pDC has not been improved by the availability of two new pDC-specific markers, mainly due to the observation that BDCA-2 Ag is down-regulated on human pDC upon activation, whereas BDCA-4 Ag is up-regulated on other DC subsets upon activation (26). The 120G8 mAb does not stain human pDC (data not shown), but our data demonstrate that this mAb can recognize both resting and activated mouse pDC, thus enabling the study of mouse pDC activation in vivo. Indeed, 120G8 expression remains stable upon pDC activation by different viral or chemical stimuli, such as LPS, influenza virus, or CpG (data not shown), in contrast to the observed BDCA-2 down-regulation expression on human pDC (26). Moreover, 120G8 does not interfere with any pDC function tested in vitro, e.g., cytokine production, survival, activation in response to viral or CpG activation, as well as T CD4$^+$ cells stimulation (data not shown), still in contrast with some anti-BDCA-2 mAbs (43). Expression of 120G8 can be up-regulated on B cells and DC upon activation, but the level of expression on those cells still remains at least one log lower than on pDC, thus still enabling pDC to be identified easily according to 120G8 high level of expression on those cells. This is in contrast with BDCA-4 Ag, which cannot be used to distinguish activated human pDC from myeloid DC. Thus 120G8 mAb is a unique tool to study mouse pDC function in vivo.

The ability of 120G8 mAb to specifically stain both resting and activated mouse pDC has enabled us to study pDC localization in different immune organs. In humans, the pDC subset has been located in the T cell area of secondary lymphoid organs, e.g., tonsil (44). However, the lack of any specific markers to activated pDC has hampered the localization of this DC subset after activation in vivo. In mice, following various viral infections, IPCs type I, later identified as pDC, have been located in the spleen marginal zone (32, 45). Data presented in this study demonstrate that in normal uninfected mice, pDC are located in the T cell area of spleen, lymph node and Peyer's patches, as well as in the red pulp, as opposed to conventional DC mainly located in the spleen marginal zone. The availability of 120G8 mAb will allow us to further elucidate whether, following in vivo activation, pDC can relocate in the spleen marginal zone (C. Asselin-Paturel, G. Brizard, and G. Trinchieri, manuscript in preparation). The discrepancy of localization between resting conventional DC and pDC further suggests differential and distinct function for those two DC subsets, in terms of T cell activation in resting conditions. Conventional DC are present in the marginal zone, ready to uptake and present any incoming Ag. In contrast, resting pDC, which have been demonstrated to display much lower ability to stimulate T cells, could circulate through the blood, playing the role of sentinels, and migrate in the spleen T cell area through arterioles or in inflamed lymph nodes through high endothelial venule, partly due to their high level of CD62L expression (46, 47).

In this report, we have performed a systematic study of three DC subsets frequency (pDC, conventional CD8$^+$ DC and CD11b$^+$ DC) in six mouse strains and six immune organs. Higher spleen pDC frequency in 129Sv mice has been previously suggested (14)

as well as the different ability of mouse strains to produce cytokines in response to similar stimuli (31). In this study, we suggest that this latter observation may be due in part to different proportion of pDC present in those distinct mouse strains. Indeed, the high ability of 129Sv mice to produce IFN-α in response to viral or bacterial stimulation can be related to their higher proportion of blood and spleen pDC, but also to the ability of pDC from 129Sv mice to produce higher levels of cytokines in response to viral stimulation, but not to bacterial stimulation. The higher production of IFN-α in response to CpG observed with 129 mice was not due to an intrinsic higher ability of mouse pDC from 129 background to secrete high levels of this cytokine. It is important to remember that many transgenic mice are bred on a mixed background between C57BL/6 and 129Sv mice. Our data imply that specific attention should be drawn to the control mice used in those studies, especially for viral and bacterial infection, because genetic background has a major effect on cytokine response in those mice. It is also important to note that many in vivo mouse infection models (e.g., *Leishmania major*) involve analysis of immune response in popliteal lymph node, following footpad injection of Ag. It still remains to be determined whether the high frequency of mouse pDC in peripheral LN from BALB/c mice could play a role in differences observed between BALB/c and other mouse strains in this model.

Our study describes the generation and use of a new mAb displaying a high specificity against both activated and resting pDC among immune cells. This Ab can be used to specifically recognize pDC and to deplete them in vivo. Thus this Ab appears to be a novel and valuable tool to elucidate mouse pDC function both in vitro and in vivo. Our data also point to the mouse strain-related discrepancy in pDC frequency and function that may be enlarged to other DC subsets. This strongly suggests that study of DC function both in viral and bacterial infections should more accurately take into account mouse strain differences. This study also proposes one additional explanation for mouse strain discrepancies observed in terms of resistance to bacterial or viral infections.

Acknowledgments

We thank Nadia Yessaad for technical assistance; Isabelle Durand for FACS sorting expertise; Anne O'Garra and Andre Boonstra for helpful discussion; and Alain Vicari for critical reading of the manuscript.

References

1. Steinman, R. M. 1991. The dendritic cell system and its role in immunogenicity. *Annu. Rev. Immunol. 9:271*.
2. Facchetti, F., E. Candiago, and W. Vermi. 1999. Plasmacytoid monocytes express IL3-receptor α and differentiate into dendritic cells. *Histopathology 35:88*.
3. Grouard, G., M. C. Rissoan, L. Filgueira, I. Durand, J. Banchereau, and Y.-J. Liu. 1997. The enigmatic plasmacytoid T cells develop into dendritic cells with interleukin (IL)-3 and CD40-ligand. *J. Exp. Med. 185:1101*.
4. Perussia, B., V. Fanning, and G. Trinchieri. 1985. A leukocyte subset bearing HLA-DR antigens is responsible for in vitro α interferon production in response to viruses. *Nat. Immun. Cell Growth Regul. 4:120*.
5. Siegal, F. P., N. Kadowaki, M. Shodell, P. A. Fitzgerald-Bocarsly, K. Shah, S. Ho, S. Antonenko, and Y.-J. Liu. 1999. The nature of the principal type 1 interferon-producing cells in human blood. *Science 284:1835*.
6. Kadowaki, N., S. Antonenko, and Y.-J. Liu. 2001. Distinct CpG DNA and polyinosinic-polycytidylic acid double-stranded RNA, respectively, stimulate $CD11c^-$ type 2 dendritic cell precursors and $CD11c^+$ dendritic cells to produce type I IFN. *J. Immunol. 166:2291*.
7. Starr, S. E., S. Bandyopadhyay, V. Shanmugam, N. Hassan, S. Douglas, S. J. Jackson, G. Trinchieri, and J. Chehimi. 1993. Morphological and functional differences between $HLA\text{-}DR^+$ peripheral blood dendritic cells and $HLA\text{-}DR^+$ IFN-α producing cells. *Adv. Exp. Med. Biol. 329:173*.
8. Rissoan, M. C., V. Soumelis, N. Kadowaki, G. Grouard, F. Brière, R. de Waal Malefyt, and Y.-J. Liu. 1999. Reciprocal control of T helper cell and dendritic cell differentiation. *Science 283:1183*.
9. Dubois, B., J. M. Bridon, J. Fayette, C. Barthelemy, J. Banchereau, C. Caux, and F. Brière. 1999. Dendritic cells directly modulate B cell growth and differentiation. *J. Leukocyte Biol. 66:224*.
10. Zitvogel, L. 2002. Dendritic and natural killer cells cooperate in the control/switch of innate immunity. *J. Exp. Med. 195:F9*.
11. Liu, Y.-J. 2001. Dendritic cell subsets and lineages, and their functions in innate and adaptive immunity. *Cell 106:259*.
12. Bandyopadhyay, S., B. Perussia, G. Trinchieri, D. S. Miller, and S. E. Starr. 1986. Requirement for $HLA\text{-}DR^+$ accessory cells in natural killing of cytomegalovirus-infected fibroblasts. *J. Exp. Med. 164:180*.
13. Asselin-Paturel, C., A. Boonstra, M. Dalod, I. Durand, N. Yessaad, C. Dezutter-Dambuyant, A. Vicari, A. O'Garra, C. Biron, F. Brière, and G. Trinchieri. 2001. Mouse type I IFN-producing cells are immature APCs with plasmacytoid morphology. *Nat. Immun. 2:1144*.
14. Nakano, H., M. Yanagita, and M. D. Gunn. 2001. $CD11c^+B220^+Gr\text{-}1^+$ cells in mouse lymph nodes and spleen display characteristics of plasmacytoid dendritic cells. *J. Exp. Med. 194:1171*.
15. Bjorck, P. 2001. Isolation and characterization of plasmacytoid dendritic cells from Flt3 ligand and granulocyte-macrophage colony-stimulating factor-treated mice. *Blood 98:3520*.
16. Brawand, P., D. R. Fitzpatrick, B. W. Greenfield, K. Brasel, C. R. Maliszewski, and T. De Smedt. 2002. Murine plasmacytoid pre-dendritic cells generated from Flt3 ligand-supplemented bone marrow cultures are immature APCs. *J. Immunol. 169:6711*.
17. Gilliet, M., A. Boonstra, C. Paturel, S. Antonenko, X. L. Xu, G. Trinchieri, A. O'Garra, and Y.-J. Liu. 2002. The development of murine plasmacytoid dendritic cell precursors is differentially regulated by FLT3-ligand and granulocyte/macrophage colony-stimulating factor. *J. Exp. Med. 195:953*.
18. Manfra, D. J., S. C. Chen, K. K. Jensen, J. S. Fine, M. T. Wiekowski, and S. A. Lira. 2003. Conditional expression of murine flt3 ligand leads to expansion of multiple dendritic cell subsets in peripheral blood and tissues of transgenic mice. *J. Immunol. 170:2843*.
19. Cella, M., F. Facchetti, A. Lanzavecchia, and M. Colonna. 2000. Plasmacytoid dendritic cells activated by influenza virus and CD40L drive a potent TH1 polarization. *Nat. Immun. 1:305*.
20. Kadowaki, N., S. Antonenko, J. Y. Lau, and Y.-J. Liu. 2000. Natural interferon α/β-producing cells link innate and adaptive immunity. *J. Exp. Med. 192:219*.
21. Fonteneau, J. F., M. Gilliet, M. Larsson, I. Dasilva, C. Munz, Y.-J. Liu, and N. Bhardwaj. 2003. Activation of influenza virus-specific $CD4^+$ and $CD8^+$ T cells: a new role for plasmacytoid dendritic cells in adaptive immunity. *Blood 101:3520*.
22. Liu, Y.-J., H. Kanzler, V. Soumelis, and M. Gilliet. 2001. Dendritic cell lineage, plasticity and cross-regulation. *Nat. Immun. 2:585*.
23. Gilliet, M., and Y.-J. Liu. 2002. Generation of human CD8 T regulatory cells by CD40 ligand-activated plasmacytoid dendritic cells. *J. Exp. Med. 195:695*.
24. Steinman, R. M., S. Turley, I. Mellman, and K. Inaba. 2000. The induction of tolerance by dendritic cells that have captured apoptotic cells. *J. Exp. Med. 191:411*.
25. Boonstra, A., C. Asselin-Paturel, M. Gilliet, C. Crain, G. Trinchieri, Y.-J. Liu, and A. O'Garra. 2003. Flexibility of mouse classical and plasmacytoid-derived dendritic cells in directing T helper type 1 and 2 cell development: dependency on antigen dose and differential Toll-like receptor ligation. *J. Exp. Med. 197:101*.
26. Dzionek, A., A. Fuchs, P. Schmidt, S. Cremer, M. Zysk, S. Miltenyi, D. W. Buck, and J. Schmitz. 2000. BDCA-2, BDCA-3, and BDCA-4: three markers for distinct subsets of dendritic cells in human peripheral blood. *J. Immunol. 165:6037*.
27. Pfeffer, L. M., C. A. Dinarello, R. B. Herberman, B. R. Williams, E. C. Borden, R. Bordens, M. R. Walter, T. L. Nagabhushan, P. P. Trotta, and S. Pestka. 1998. Biological properties of recombinant α-interferons: 40th anniversary of the discovery of interferons. *Cancer Res. 58:2489*.
28. van den Broek, M., U. Muller, S. Huang, R. Zinkernagel, and M. Auget. 1995. Immune defense in mice lacking type I and/or type II interferon receptors. *Immunol. Rev. 148:5*.
29. Farkas, L., K. Beiske, F. Lund-Johansen, P. Brandtzaeg, and F. L. Jahnsen. 2001. Plasmacytoid dendritic cells (natural interferon-α/β-producing cells) accumulate in cutaneous lupus erythematosus lesions. *Am. J. Pathol. 159:237*.
30. Jahnsen, F. L., F. Lund-Johansen, J. F. Dunne, L. Farkas, R. Haye, and P. Brandtzaeg. 2000. Experimentally induced recruitment of plasmacytoid ($CD123^{high}$) dendritic cells in human nasal allergy. *J. Immunol. 165:4062*.
31. Dalod, M., T. P. Salazar-Mather, L. Malmgaard, C. Lewis, C. Asselin-Paturel, F. Brière, G. Trinchieri, and C. A. Biron. 2002. Interferon α/β and interleukin 12 responses to viral infections: pathways regulating dendritic cell cytokine expression in vivo. *J. Exp. Med. 195:517*.
32. Barchet, W., M. Cella, B. Odermatt, C. Asselin-Paturel, M. Colonna, and U. Kalinke. 2002. Virus-induced interferon α production by a dendritic cell subset in the absence of feedback signaling in vivo. *J. Exp. Med. 195:507*.
33. Hestdal, K., F. W. Ruscetti, J. N. Ihle, S. E. Jacobsen, C. M. Dubois, W. C. Kopp, D. L. Longo, and J. R. Keller. 1991. Characterization and regulation of RB6–8C5 antigen expression on murine bone marrow cells. *J. Immunol. 147:22*.
34. Fleming, T. J., M. L. Fleming, and T. R. Malek. 1993. Selective expression of Ly-6G on myeloid lineage cells in mouse bone marrow. RB6–8C5 mAb to granulocyte-differentiation antigen (Gr-1) detects members of the Ly-6 family. *J. Immunol. 151:2399*.
35. Jutila, M. A., F. G. Kroese, K. L. Jutila, A. M. Stall, S. Fiering, L. A. Herzenberg, E. L. Berg, and E. C. Butcher. 1988. Ly-6C is a monocyte/macrophage and endothelial cell differentiation antigen regulated by interferon-γ. *Eur. J. Immunol. 18:1819*.
36. Takahama, Y., S. O. Sharrow, and A. Singer. 1991. Expression of an unusual T cell receptor (TCR)-Vβ repertoire by $Ly\text{-}6C^+$ subpopulations of $CD4^+$ and/or $CD8^+$ thymocytes: evidence for a developmental relationship between $Ly\text{-}6C^+$ thymocytes and $CD4^-CD8^-$ TCR-α/β^+ thymocytes. *J. Immunol. 147:2883*.
37. Sato, N., T. Yahata, K. Santa, A. Ohta, Y. Ohmi, S. Habu, and T. Nishimura. 1996. Functional characterization of $NK1.1^+$ $Ly\text{-}6C^+$ cells. *Immunol. Lett. 54:5*.

38. O'Keeffe, M., H. Hochrein, D. Vremec, I. Caminschi, J. L. Miller, E. M. Anders, L. Wu, M. H. Lahoud, S. Henri, B. Scott, P. Hertzog, L. Tatarczuch, and K. Shortman. 2002. Mouse plasmacytoid cells: long-lived cells, heterogeneous in surface phenotype and function, that differentiate into $CD8^+$ dendritic cells only after microbial stimulus. *J. Exp. Med. 196:1307*.

39. Dalod, M., T. Hamilton, R. Salomon, T. P. Salazar-Mather, S. C. Henry, J. D. Hamilton, and C. A. Biron. 2003. Dendritic cell responses to early murine cytomegalovirus infection: subset functional specialization and differential regulation by interferon α/β. *J. Exp. Med. 197:885*.

40. Edwards, A. D., S. S. Diebold, E. M. Slack, H. Tomizawa, H. Hemmi, T. Kaisho, S. Akira, and C. Reis e Sousa. 2003. Toll-like receptor expression in murine DC subsets: lack of TLR7 expression by $CD8\alpha^+$ DC correlates with unresponsiveness to imidazoquinolines. *Eur. J. Immunol. 33:827*.

41. Edwards, A. D., S. P. Manickasingham, R. Sporri, S. S. Diebold, O. Schulz, A. Sher, T. Kaisho, S. Akira, and C. Reis e Sousa. 2002. Microbial recognition via Toll-like receptor-dependent and -independent pathways determines the cytokine response of murine dendritic cell subsets to CD40 triggering. *J. Immunol. 169:3652*.

42. Moser, M., and K. M. Murphy. 2000. Dendritic cell regulation of TH1-TH2 development. *Nat. Immun. 1:199*.

43. Dzionek, A., Y. Sohma, J. Nagafune, M. Cella, M. Colonna, F. Facchetti, G. Gunther, I. Johnston, A. Lanzavecchia, T. Nagasaka, et al. 2001. BDCA-2, a novel plasmacytoid dendritic cell-specific type II C-type lectin, mediates antigen capture and is a potent inhibitor of interferon α/β induction. *J. Exp. Med. 194:1823*.

44. Summers, K. L., B. D. Hock, J. L. McKenzie, and D. N. Hart. 2001. Phenotypic characterization of five dendritic cell subsets in human tonsils. *Am. J. Pathol. 159:285*.

45. Eloranta, M. L., and G. V. Alm. 1999. Splenic marginal metallophilic macrophages and marginal zone macrophages are the major interferon-α/β producers in mice upon intravenous challenge with herpes simplex virus. *Scand. J. Immunol. 49:391*.

46. Cella, M., D. Jarrossay, F. Facchetti, O. Alebardi, H. Nakajima, A. Lanzavecchia, and M. Colonna. 1999. Plasmacytoid monocytes migrate to inflamed lymph nodes and produce large amounts of type I interferon. *Nat. Med. 5:919*.

47. Penna, G., S. Sozzani, and L. Adorini. 2001. Cutting edge: selective usage of chemokine receptors by plasmacytoid dendritic cells. *J. Immunol. 167:1862*.